https://doi.org/10.5194/egusphere-2026-1314
Preprint. Discussion started: 15 June 2026

A dense rain-gauge observation framework for advection-consistency diagnosis of urban convective rainfall

Punpiti Piamsa-nga[1], Nalina Phisanbut[1], and Napaporn Piamsa-nga[2]

[1]Department of Computer Engineering, Kasetsart University, 50 Ngamwongwan Rd., Ladyao, Chatuchak, Bangkok 10900, Thailand
[2]Department of Water Resources Engineering, Kasetsart University, 50 Ngamwongwan Rd., Ladyao, Chatuchak, Bangkok 10900, Thailand

Correspondence: Napaporn Piamsa-nga (napaporn.r@ku.th)

Abstract. Convective rainfall identification is commonly based on intensity thresholds, radar reflectivity patterns, or supervised classification methods. However, these approaches often lack an explicit connection to the physical constraints governing rainfall-field evolution. This study proposes a physics-informed definition of convective rainfall based on the continuity equation, interpreting convective rainfall as a spatiotemporal deviation from rainfall evolution consistent with horizontal advection under the rainfall continuity equation.

The analysis utilizes data from a high-density rain gauge network in Bangkok. Rainfall fields are reconstructed on a kilometer-scale grid, and the motion field is estimated using the Horn-Schunck optical flow method under no-flux boundary conditions. The rainfall field is then advected forward in time without including local source or sink terms. The residual between the observed field and the purely advected field is interpreted as representing non-advective processes. The framework is designed for dense urban rain-gauge networks, where direct surface rainfall measurements are available and quantitatively calibrated radar rainfall products are not available for the present analysis.

Residual-feature analyses indicate that the detected events exhibit properties consistent with convective rainfall, including spatial localization, rapid development, and a clear association with the diurnal cycle. The separation between convective and non-convective events in the residual feature space provides an empirical evaluation of the diagnostic behavior of the framework.

The results suggest that advection consistency provides an interpretable physics-based foundation for defining and detecting convective rainfall using rain gauge observations alone.

1 Introduction

Convective rainfall is one of the most dynamically active forms of precipitation, characterized by rapid initiation, strong spatial localization, and short lifetimes, particularly in tropical and subtropical regions (Wang et al., 2021). Such phenomena are of critical importance for large metropolitan areas, where highly localized and intense rainfall can lead to flash flooding and infrastructure risks within short time scales (Caseri et al., 2022; Li et al., 2024; Gu et al., 2025).

https://doi.org/10.5194/egusphere-2026-1314
Preprint. Discussion started: 15 June 2026

In many tropical cities, rainfall monitoring systems still rely primarily on dense ground-based rain gauge networks. Although weather radar provides spatially continuous observations, its availability, coverage, or resolution may be limited in certain contexts. Rain gauge networks offer high temporal accuracy but inherently lack spatial continuity, making the interpretation of convective rainfall based solely on station observations a methodological challenge.

The emphasis on rain gauge observations is not intended to imply that radar data are unsuitable for rainfall monitoring. Radar observations provide spatially continuous information and are central to many rainfall nowcasting systems. However, radar-derived rainfall products are indirect estimates and require local calibration against surface rainfall observations; otherwise, reflectivity-based products may be affected by calibration uncertainty, attenuation, beam blockage, vertical-profile effects, and assumptions in the reflectivity-rainfall relationship (Villarini and Krajewski, 2010; Berne and Krajewski, 2013). Although the available radar imagery may have fine nominal spatial sampling, nominal pixel spacing alone does not ensure quantitative rainfall accuracy at the surface. In the Bangkok setting considered here, a quantitatively calibrated radar rainfall product was not available for the present analysis. The present study therefore develops a complementary framework based on dense surface gauge observations, rather than a replacement for radar-based approaches.

Previous studies have typically identified convective rainfall using rainfall intensity thresholds, radar reflectivity structures, or expert classification (Anagnostou, 2004; Feidas and Giannakos, 2012; Giannakos and Feidas, 2013; Wang et al., 2021). While such approaches are useful within specific observational systems, they often depend on instrument-specific characteristics and lack a physics-based interpretative framework directly linked to the dynamical evolution of rainfall fields.

Despite these advances, a clear operational definition of convective rainfall grounded in physical principles and directly applicable to rain gauge data remains limited. This study adopts a different perspective: rather than defining convective rainfall purely by intensity, it interprets convective rainfall as a dynamical deviation from rainfall evolution that is consistent with horizontal advection.

Within this framework, rainfall evolution can be described using the continuity equation, which separates advective transport from source-sink processes. If a physically constrained motion field is estimated from rain gauge data and used to advect the rainfall field forward in time, the discrepancy between the observed field and the purely advected field can be interpreted as a signal of non-advective processes, such as local convective initiation.

The methodological contribution of this study is a measurement-based framework for diagnosing urban rainfall-system evolution from dense rain-gauge observations. The workflow consists of four linked components: (1) organizing station-scale rainfall records into storm systems, (2) reconstructing gauge-derived rainfall fields on a kilometer-scale grid, (3) estimating an advection-consistent motion field from the reconstructed rainfall fields, and (4) using the residual between the observed and advected rainfall fields as a diagnostic indicator of local rainfall growth not explained by horizontal transport. This design converts direct surface rainfall measurements into a process-oriented diagnostic quantity and is intended for urban regions where dense gauge networks are already available.

Based on this principle, the present study applies the framework to high-resolution rain gauge observations in the Bangkok metropolitan area as a dense urban gauge-network test case. The framework is evaluated through event-based analyses and statistical characteristics of the detected rainfall events. The results indicate that the identified events exhibit meteorological

https://doi.org/10.5194/egusphere-2026-1314
Preprint. Discussion started: 15 June 2026

properties consistent with convective rainfall, including spatial localization, rapid development, and association with the diurnal cycle. These findings suggest that advection consistency provides an interpretable physics-based basis for defining and detecting convective rainfall using rain gauge observations alone.

2 Literature review

Short-term rainfall analysis and forecasting constitute important research topics in meteorology and hydrology because precipitation is a phenomenon characterized by high variability in both time and space (Nakaegawa et al., 2019; Mu et al., 2021; Xiao et al., 2018; Zhuo et al., 2014). For the purposes of this review, existing approaches to describing or predicting the evolution of rainfall fields are grouped into three main categories: (1) data-driven approaches, (2) advection-based approaches that assume the motion of precipitation structures, and (3) anomaly-based detection methods that identify rainfall events from deviations in atmospheric variables.

2.1 Data-driven precipitation modeling

Over the past decade, the use of machine learning and deep learning for rainfall prediction has gained significant attention (Das et al., 2017; Caseri et al., 2022; Ha and Lee, 2024; He et al., 2023; Lazri and Ameur, 2018), as these methods can directly learn complex relationships between atmospheric variables and rainfall amounts. For example, convolutional recurrent neural networks have been used to forecast rainfall from radar observations (Caseri et al., 2022), while architectures incorporating attention mechanisms have been proposed to enhance the ability of models to learn spatial and temporal dependencies associated with heavy rainfall events (Zhao et al., 2024).

However, purely data-driven approaches often do not explicitly account for the physical constraints of the atmospheric system. As a result, such models may achieve high accuracy on training data but may not adequately explain the underlying mechanisms of the system or generalize well to new events. This limitation has motivated the development of physics-informed machine learning, which aims to integrate physical knowledge with data-driven models in order to ensure that the resulting predictions remain consistent with the fundamental laws governing natural systems (Kashinath et al., 2021; Bhasme et al., 2022; Luo et al., 2025; Teufel et al., 2023; Karpatne et al., 2017; Abbasi et al., 2024).

In hydrological applications, this concept has been applied to improve the representation of hydrological processes by combining the structure of physically based models with machine learning, thereby enhancing both predictive accuracy and physical consistency (Xie et al., 2021). Recent studies have also explored the use of physics-guided learning for the prediction of heavy rainfall events by incorporating atmospheric dynamical information into machine learning models to improve forecasting performance (Zhong et al., 2024; Das et al., 2024).

Although these approaches improve the physical consistency of data-driven models, they generally remain focused on statistical prediction rather than on directly analyzing the dynamical structure of rainfall fields.

https://doi.org/10.5194/egusphere-2026-1314
Preprint. Discussion started: 15 June 2026

2.2 Advection-based rainfall evolution models

Another important approach in short-term rainfall forecasting assumes that changes in rainfall fields over short time intervals can be explained primarily by advection, or the horizontal transport of precipitation structures (Bowler et al., 2004; Muñoz et al., 2018). This concept is based on the assumption that the spatial pattern of rainfall can be transported by the atmospheric velocity field while largely preserving its main structure over short lead times.

Methods based on this concept typically employ optical flow or echo-tracking techniques to estimate the motion field of precipitation from sequences of radar or satellite images, which is then used to predict the future location of rainfall (Bowler et al., 2004; Muñoz et al., 2018; Ha and Lee, 2024; Smith et al., 2024). Such techniques have demonstrated strong predictive performance for short lead times, particularly during the first few hours of forecasting (Bowler et al., 2004; Ha and Lee, 2024; Smith et al., 2024).

However, the advection assumption has important limitations. The evolution of rainfall fields is not governed solely by the movement of existing precipitation structures, but also involves atmospheric dynamical processes such as the initiation of new convective cells, the intensification of precipitation, and the dissipation of rainfall systems. These processes cannot be fully explained by kinematic transport alone.

Recent studies have attempted to extend this framework by combining optical flow with deep learning in order to better capture complex motion patterns within precipitation systems (Ha and Lee, 2024). Nevertheless, these approaches still primarily rely on advection as the main mechanism for describing the evolution of rainfall.

2.3 Anomaly-based detection of rainfall events

Another approach for detecting rainfall events is the analysis of anomalies, or deviations of atmospheric variables from their normal conditions (Li et al., 2022b). The fundamental idea behind this class of methods is that rainfall events, particularly heavy rainfall, are often associated with unusual changes in certain meteorological variables prior to or during the occurrence of precipitation (Li et al., 2022a).

For example, several studies have used anomalies in precipitable water vapor (PWV) derived from GNSS observations to identify heavy rainfall events by comparing current values with their climatological or statistical norms (Li et al., 2022b, a). Such methods can detect atmospheric conditions favorable for rainfall in advance, as atmospheric moisture content is a key variable controlling the potential for precipitation formation.

Related detection and estimation studies have also used multiple atmospheric predictors, including GNSS-derived PWV and zenith total delay variables, microwave-radiometer brightness temperatures related to atmospheric temperature and humidity, and satellite or reanalysis features such as column water vapor, black-body temperature, and cloud-base height (Li et al., 2022b, a; Das et al., 2017; He et al., 2023). These approaches often employ statistical analysis or machine learning techniques to identify atmospheric patterns associated with rainfall events.

https://doi.org/10.5194/egusphere-2026-1314
Preprint. Discussion started: 15 June 2026

However, although anomaly-based methods can effectively detect rainfall events from a statistical perspective, they generally do not explicitly link the detection process to the physical mechanisms governing the evolution of rainfall fields (Xie et al., 2021; Bhasme et al., 2022).

Beyond studies that focus directly on rainfall prediction or event detection, climatological analyses have examined statistical characteristics of precipitation, including the frequency, intensity, and diurnal cycle of rainfall (Nakaegawa et al., 2019; Xiao et al., 2018; Zhuo et al., 2014; Zhao et al., 2022; Gu et al., 2025). Such studies improve our understanding of long-term rainfall patterns and provide important background information for the development and evaluation of forecasting models.

2.4 Statistical characterization of rainfall variability

Related climatological studies have examined statistical characteristics of precipitation, such as the diurnal cycle of rainfall, as well as the frequency and intensity of precipitation across different regions (Nakaegawa et al., 2019; Xiao et al., 2018; Zhuo et al., 2014; Zhao et al., 2022; Gu et al., 2025). These studies include both temperate and tropical regions and often rely on observations from rain gauge stations, radar systems, or satellite measurements to analyze the temporal and spatial patterns of precipitation (Mu et al., 2021). These investigations contribute to a deeper understanding of the climatological characteristics of rainfall, including diurnal patterns, seasonal variability, and the frequency of heavy precipitation events. They also play an important role in evaluating the consistency and performance of climate models and numerical weather prediction systems (Mu et al., 2021).

Although these approaches have significantly advanced the analysis and prediction of rainfall, they emphasize different aspects of the precipitation process. Data-driven models focus on statistical relationships between atmospheric variables and rainfall, advection-based approaches describe the kinematic transport of existing precipitation structures, and anomaly-based methods identify atmospheric conditions associated with rainfall events. Studies on rainfall variability, meanwhile, provide important climatological context for understanding precipitation patterns across different spatial and temporal scales. However, these approaches generally do not explicitly examine the physical consistency of rainfall evolution with respect to the underlying transport dynamics of the precipitation field. In particular, the extent to which observed changes in rainfall can be explained solely by horizontal advection, or instead reflect local generation or decay processes, remains less directly quantified in existing frameworks.

In this study, we address this gap by introducing a physics-based framework for analyzing rainfall evolution using the continuity equation. By evaluating the residual between the observed temporal change of rainfall and the change expected from advection, the proposed approach provides a physically interpretable indicator of rainfall dynamics. This formulation enables the identification of rainfall components that are dynamically inconsistent with advection, which we interpret as signatures of convective processes. The framework therefore offers a complementary perspective to existing statistical and kinematic approaches for rainfall analysis and detection.

https://doi.org/10.5194/egusphere-2026-1314
Preprint. Discussion started: 15 June 2026

3 Data and study area

3.1 Study area and climatic context

The study area covers the Bangkok Metropolitan Region and its surrounding areas in central Thailand. The region is situated on a low-lying alluvial delta plain characterized by minimal topographic gradients and a densely developed drainage infrastructure.

The urban core spans approximately 1,500 km^2 and extends continuously into surrounding peri-urban zones, as shown in Fig. 1 (a). The network provides a dense long-term urban rain-gauge dataset, enabling kilometer-scale rainfall analysis without reliance on radar observations. Among the 130 geolocated stations, the median nearest-neighbor station spacing is approximately 1.5 km (interquartile range 0.8–2.4 km), with a mean nearest-neighbor spacing of approximately 1.9 km.

The regional climate is governed by two primary monsoon systems. The southwest monsoon, active from May to October, brings moist air masses and is associated with intense rainfall events. In contrast, the northeast monsoon, from November to February, is comparatively dry. Transitional periods between these seasons frequently produce convective thunderstorms with pronounced local characteristics, providing an appropriate context for studying short-lived and spatially localized rainfall events.

3.2 Rain-gauge network and data characteristics

The rainfall data are obtained from a network of 131 automatic rain-gauge stations operated by the Bangkok Metropolitan Administration. The spatial distribution of stations is illustrated in Fig. 1 (b), with high density in the inner urban area and decreasing coverage toward the periphery due to installation constraints.

The dataset spans the period 2000–2024 and is recorded at a consistent temporal resolution of 15 min. This long-term, high-frequency dataset is well suited for analyzing rapidly evolving and short-lived rainfall dynamics. The station density in the urban area supports the construction of kilometer-scale spatial rainfall fields without relying on excessive long-distance interpolation. Nevertheless, the siting of stations—often located at public facilities or hydraulic structures—should be considered when interpreting the spatial representativeness of the observations.

3.3 Data quality control and dataset characteristics

All rainfall records underwent basic quality assurance and quality control procedures, including the marking of outliers, correction of duplicated timestamps, and temporal alignment across stations to ensure consistency at the 15-min resolution throughout the study period. Outliers were identified using physically plausible limits for 15-min rainfall accumulation together with temporal consistency checks between adjacent observations. Records exceeding these physically plausible limits were removed during the QA/QC process.

Because rainfall is highly intermittent at the 15-min resolution, only a small fraction of time steps contain measurable rainfall. Across all stations, approximately 6% of the observations correspond to non-zero rainfall after QA/QC, while the remaining intervals represent dry conditions rather than missing data, as summarized in Table 1. The dataset is temporally

https://doi.org/10.5194/egusphere-2026-1314
Preprint. Discussion started: 15 June 2026

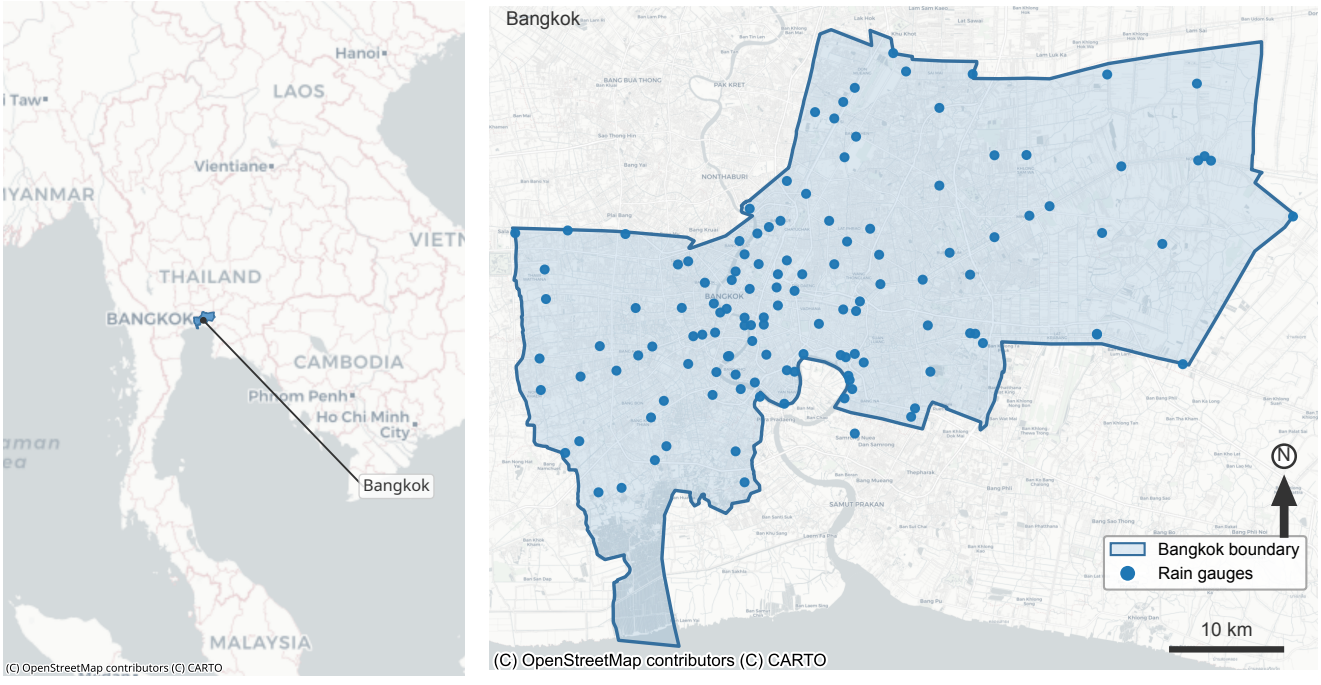

(a) **(b)**

Figure 1. Location of the Bangkok Metropolitan Region within Thailand (a) and distribution of the 131 automatic rain-gauge stations operated by the Bangkok Metropolitan Administration (BMA) (b). Station density is highest in the urban core and decreases toward peri-urban areas due to siting constraints at public facilities and hydraulic structures.

aligned such that each time step corresponds to a 15-min accumulation period, ensuring that rainfall fields can be compared consistently between consecutive time steps for motion estimation.

Rainfall events were defined as continuous periods with rainfall greater than zero, allowing short dry gaps below a predefined threshold to avoid artificially splitting physically coherent rainfall systems. This definition reflects the structural continuity of rainfall at the event scale rather than segmenting events solely based on instantaneous observations.

3.4 Spatial field reconstruction (data gridding)

To enable spatial analysis of rainfall motion, point-based rain-gauge observations were mapped onto a Cartesian grid with a spatial resolution of $1 \times 1\,\mathrm{km}^2$. Rainfall values within each grid cell were obtained by aggregating all stations located inside the cell. When multiple stations were present within the same grid cell, their mean rainfall value was used as the representative rainfall intensity for that cell.

https://doi.org/10.5194/egusphere-2026-1314
Preprint. Discussion started: 15 June 2026

Table 1. Summary statistics of the BMA rain-gauge dataset after quality control (2000–2024). Station-level statistics are reported as mean, minimum, and maximum across 131 stations.

	Station statistics		
Metric	Mean	Min	Max
Records per station (raw)	99 026	99 014	99 039
Non-zero rainfall observations (%)	6.39	1.48	9.22
Zero-rainfall observations (%)	93.61	90.78	98.52
Records flagged as outliers during QA/QC (%)	34.79	8.86	86.09
Dataset-level metrics			
Temporal coverage with ≥90% stations (%)		35.70	
Number of stations		131	

Grid cells without stations were initially treated as missing values. No long-range spatial interpolation (e.g., inverse-distance weighting or kriging) was applied, because the objective of the gridding procedure was not to reconstruct a complete rainfall surface, but to preserve the local spatial structure of the gauge observations.

The choice of kilometer-scale resolution was guided by the station density in the Bangkok Metropolitan Region, where the urban gauge network provides sufficient coverage to represent rainfall structures at this scale without requiring strong long-distance interpolation. This resolution is appropriate for capturing rainfall cell structures relevant to urban-scale convective processes and short-term motion estimation.

An example of the computational grid and station-to-cell mapping is shown in Fig. 2. The resulting gridded field provides the spatial basis for the rainfall representation developed in Section 4.

4 Rainfall representation for physics-based analysis

The physical analysis of rainfall motion and evolution requires rainfall to be represented as a spatial field in which temporal and spatial derivatives can be defined. However, the original observations in this study consist of discrete point measurements from rain gauges. Therefore, before estimating rainfall motion, the gauge observations must be converted into a spatial representation suitable for dynamical analysis.

The gridded rainfall field introduced in Section 3.4 provides the initial spatial structure for this representation. Because rain-gauge observations are discrete, the resulting field may still contain spatial discontinuities. For motion estimation and residual analysis, the field is therefore regularized through spatial smoothing to obtain a spatially coherent and differentiable rainfall representation.

The objective of this representation is not to reconstruct detailed point-level rainfall estimates, but to retain the dominant rainfall distribution patterns at a scale appropriate for motion estimation and continuity-equation-based analysis. This repre-

https://doi.org/10.5194/egusphere-2026-1314
Preprint. Discussion started: 15 June 2026

sentation makes it possible to distinguish rainfall evolution associated with horizontal transport from that associated with local source-sink behavior.

4.1 Gridded rainfall field

The rainfall field used in the subsequent analysis was constructed from the gridded gauge observations described in Section 3.4. Rainfall values were assigned to $1 \times 1\,\mathrm{km}^2$ grid cells using cell-based aggregation of the stations located within each cell. When multiple stations were present in the same cell, their mean rainfall value was used as the primary representation.

This gridded field preserves the original observational structure of the gauge network and avoids imposing long-range interpolation assumptions. However, because the gauge observations are discrete, the resulting field may contain gaps and sharp spatial discontinuities that are not suitable for direct derivative-based analysis. The gridded field should therefore be regarded as the observational basis of the rainfall representation rather than the final analysis-ready field.

Figure 2 illustrates the computational grid and the mapping of rain-gauge locations onto the analysis domain. This gridded representation serves as the starting point for the spatial regularization step described in the following subsection.

4.2 Spatiotemporal consistency of the dataset

Prior to field reconstruction, the rain-gauge data were prepared to ensure temporal alignment and network-wide comparability. All stations were synchronized to common 15-min accumulation intervals, so that each time step represents rainfall accumulated over the same duration across the entire observation network. Basic quality control was also applied to remove anomalous values and preserve temporal continuity.

Temporal synchronization and the availability of observations from most stations at each 15-min time step are essential for motion estimation, because optical flow methods infer displacement by comparing rainfall patterns between consecutive fields. These preparation steps produced a rain-gauge dataset with sufficient spatiotemporal coherence for short-term motion estimation and for the subsequent analysis of advection consistency.

5 Estimation of advection-consistent motion

To establish a physics-based reference for assessing whether rainfall evolution is governed primarily by horizontal advection, it is first necessary to estimate the motion field that transports rainfall structures between consecutive time steps. The objective is not to perform operational forecasting, but rather to construct a physically interpretable motion field that represents the displacement of rainfall patterns over short temporal intervals.

In this study, the motion field is estimated between consecutive rainfall maps separated by $\Delta t = 15\,\mathrm{min}$. This relatively short interval is chosen to ensure that the assumption of advection-dominated evolution remains physically reasonable. Over such time scales, large-scale rainfall structures typically move coherently with the ambient flow, while microphysical growth and decay processes occur more gradually.

https://doi.org/10.5194/egusphere-2026-1314
Preprint. Discussion started: 15 June 2026

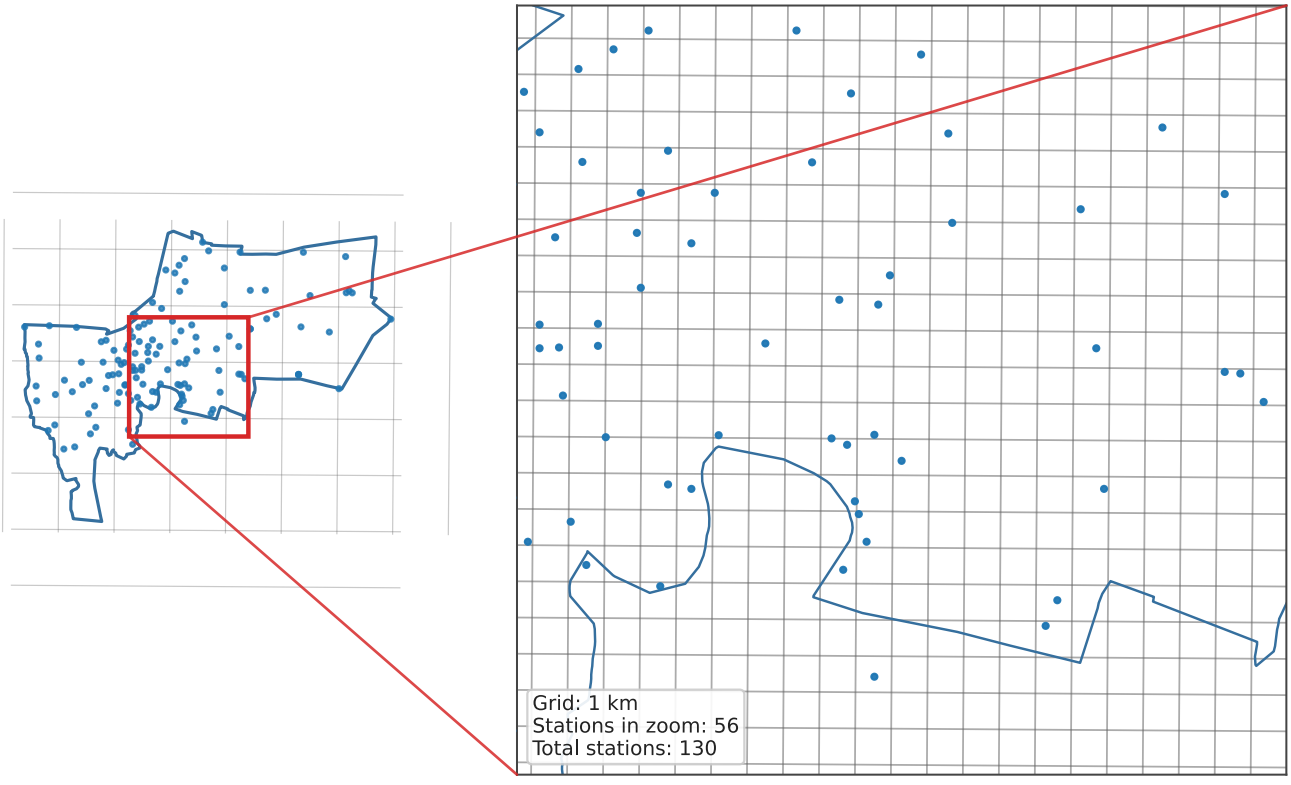

Figure 2. Example of the 1×1 km^2 computational grid used for rainfall analysis. Blue dots denote rain-gauge stations, and gray lines indicate the spatial discretization of the analysis domain. When multiple stations fall within the same grid cell, their rainfall values are aggregated using the mean to represent the cell intensity.

Let $R(x,y,t)$ denote rainfall intensity defined on a spatial grid. The horizontal motion field describing the displacement of rainfall structures is denoted by

$$\mathbf{V}(x,y,t) = (u(x,y,t), v(x,y,t)),$$

where u and v represent the zonal and meridional components of the motion field, respectively.

The goal of motion estimation is therefore to determine $\mathbf{V}$ such that the observed evolution of the rainfall field between t and $t+\Delta t$ can be explained as the advection of rainfall structures by this velocity field. This estimated motion field will then serve as the basis for advecting the rainfall field forward in time and assessing the consistency of observed evolution with advection.

https://doi.org/10.5194/egusphere-2026-1314
Preprint. Discussion started: 15 June 2026

5.1 Optical flow formulation

Rainfall motion is estimated using the Horn-Schunck optical flow method (Horn and Schunck, 1981), treating rainfall intensity as a scalar field transported by a horizontal velocity field. This formulation originates from computer vision, but is physically consistent with the advection of passive scalars in fluid dynamics.

Under the short-term brightness constancy assumption, rainfall intensity is assumed to be conserved along motion trajectories:

$$R(x,y,t) = R(x+u\Delta t,\, y+v\Delta t,\, t+\Delta t).$$

This assumption implies that changes in rainfall intensity at a fixed location arise primarily from the movement of existing precipitation structures rather than from local generation or dissipation processes.

Figure 3 illustrates an example of rainfall evolution together with the estimated motion field. Panel (a) shows the rainfall field at time t, panel (b) displays the estimated motion vectors describing the displacement of rainfall structures between the two time steps, and panel (c) shows the observed rainfall field at time $t+\Delta t$. The estimated vectors capture coherent spatial patterns consistent with the displacement of rainfall features across the domain.

Under the brightness constancy assumption, the temporal change of rainfall intensity is constrained by the advection equation. Linearizing the above relation yields the classical optical flow constraint equation

$$\frac{\partial R}{\partial t} + u\frac{\partial R}{\partial x} + v\frac{\partial R}{\partial y} = 0 \tag{1}$$

Physically, Eq. (1) expresses conservation of rainfall intensity along the trajectories defined by the motion field. In other words, rainfall behaves locally as a passive scalar advected by the horizontal flow.

However, Eq. (1) contains two unknown velocity components (u, v) but only one constraint equation. To obtain a unique and physically meaningful solution, a variational framework is adopted.

Specifically, the Horn-Schunck method determines the velocity field by minimizing the following energy functional:

$$E(u,v) = \iint \Big(\frac{\partial R}{\partial t} + uR_x + vR_y\Big)^2 + \alpha^2\Big(|\nabla u|^2 + |\nabla v|^2\Big)\, dx\, dy \tag{2}$$

In Eq. (2), the first term enforces consistency with the optical flow constraint expressed in Eq. (1). This term penalizes deviations from the advection assumption.

The second term imposes a spatial smoothness constraint on the velocity field. The parameter α controls the relative strength of this regularization. Physically, this smoothness assumption reflects the fact that rainfall systems at urban scales tend to exhibit coherent motion driven by larger-scale atmospheric flow rather than independent pixel-scale displacements.

Figure 3 shows an example of the estimated motion field obtained using this approach. The vector field reveals spatially coherent motion patterns that characterize the displacement of rainfall structures over the study region.

https://doi.org/10.5194/egusphere-2026-1314
Preprint. Discussion started: 15 June 2026

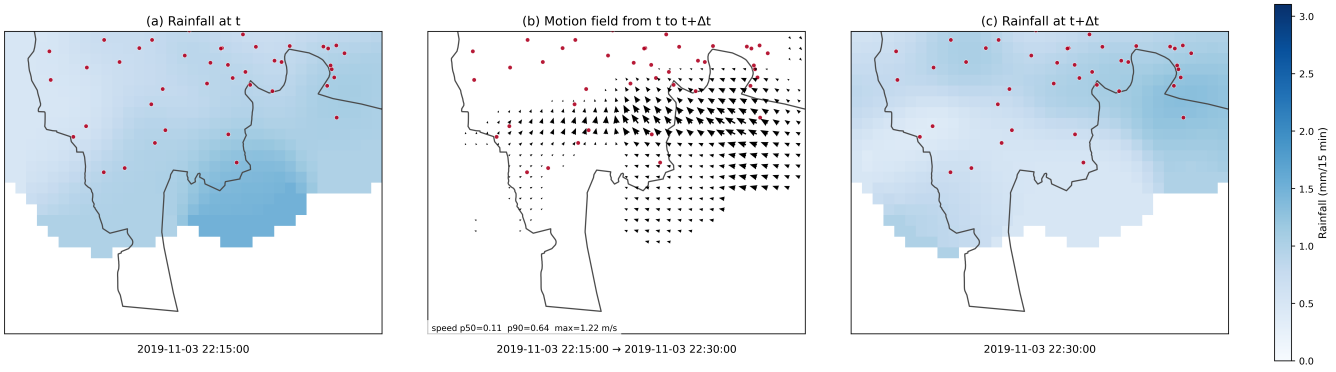

Figure 3. Example of rainfall evolution and the corresponding estimated motion field. (a) Rainfall intensity at time t. (b) Estimated horizontal velocity field describing the displacement of rainfall structures from t to $t+\Delta t$. (c) Observed rainfall field at time $t+\Delta t$. The figure illustrates how the estimated motion vectors capture the spatial displacement of rainfall features between consecutive observation times.

5.2 Boundary conditions

To avoid artificial inflow or outflow of rainfall motion at the boundaries of the computational domain, zero-flux (Neumann) boundary conditions are imposed on the velocity field:

$$\frac{\partial u}{\partial n} = 0, \qquad \frac{\partial v}{\partial n} = 0,$$

where $\frac{\partial}{\partial n}$ denotes the derivative normal to the domain boundary.

These boundary conditions prevent the introduction of artificial gradients in the estimated motion field near the domain boundaries.

Consequently, deviations from advection detected in subsequent analyses can be interpreted as intrinsic evolution of the rainfall system rather than artifacts produced by boundary effects.

5.3 Advection-only rainfall evolution

Once the motion field $\mathbf{V} = (u, v)$ has been estimated, the rainfall intensity field can be advected forward in time using the linear advection equation

$$\frac{\partial R}{\partial t} + \mathbf{V} \cdot \nabla R = 0.$$

This equation describes the transport of a passive scalar by a prescribed velocity field. In the present study, rainfall intensity is treated as a scalar field that is transported horizontally by the estimated motion field.

Let $R_{\mathrm{obs}}(x, y, t)$ denote the observed rainfall field, a spatial rainfall intensity field defined on the analysis grid. Because rainfall observations are available only at discrete rain gauge locations, the gridded rainfall field is constructed by aggregating gauge measurements within each grid cell of the computational grid. Consequently, $R_{\mathrm{obs}}(x, y, t)$ should be interpreted as a grid-based representation derived from gauge observations rather than direct measurements at every grid cell.

https://doi.org/10.5194/egusphere-2026-1314
Preprint. Discussion started: 15 June 2026

In discrete form, the advected rainfall field at time $t + \Delta t$ can be approximated as

$$R_{\mathrm{adv}}(x, y, t + \Delta t) = R_{\mathrm{obs}}(x, y, t) - \Delta t \left(u \frac{\partial R_{\mathrm{obs}}}{\partial x} + v \frac{\partial R_{\mathrm{obs}}}{\partial y} \right).$$

In this formulation, no additional source or sink terms are included. The predicted field R_{adv} therefore represents rainfall evolution under pure horizontal advection alone, assuming that rainfall structures are transported without local growth or decay.

The velocity field used in the advection step corresponds to the motion field estimated from consecutive rainfall fields, as illustrated in Fig. 3 (b). Using this motion field, the rainfall distribution at time t can be advected forward to obtain the rainfall field expected at time $t + \Delta t$ under the assumption of purely advective transport.

Advection-based extrapolation is applied only over short lead times not exceeding 60 min. This limitation helps maintain the validity of the linear advection assumption and reduces the accumulation of errors associated with rainfall growth, decay, and microphysical processes that are not represented in the advection model.

Importantly, the purpose of this advection-only prediction is not to produce an operational rainfall forecast. Instead, it provides a physically interpretable baseline representing the rainfall field expected if horizontal transport were the dominant mechanism governing rainfall evolution.

An example comparison between the advected rainfall field and the rainfall field derived from gauge observations at the subsequent time step is shown in Fig. 4. The comparison includes the rainfall field at time t, the rainfall field advected forward using the estimated motion field, and the reconstructed rainfall field at time $t + \Delta t$ obtained from gauge observations.

By comparing the advected rainfall field with the observed rainfall field at $t + \Delta t$, it becomes possible to identify regions where rainfall evolution deviates from the behavior expected under pure advection. Such deviations indicate the presence of local rainfall growth or decay processes that cannot be explained solely by horizontal transport.

In this example, the advected rainfall field appears visually similar to the rainfall field at time t. This is expected because the estimated displacement during the 15-min interval is generally smaller than the grid spacing, resulting in sub-pixel advection shifts. The rainfall field used for motion estimation is also spatially regularized through local smoothing in order to obtain a spatially coherent and differentiable rainfall field suitable for optical flow estimation and stable spatial derivative computation. Consequently, the difference between the advected and observed rainfall fields becomes more clearly expressed in the residual panel (Fig. 4 (d)), which highlights rainfall growth and decay not explained by horizontal advection.

The relationship between rainfall evolution and the estimated motion field can be further illustrated by examining consecutive rainfall maps together with the inferred velocity vectors. Figure 5 presents an example in which the rainfall field at time t, the estimated motion field between the two observation times, and the rainfall field at time $t + \Delta t$ are shown together.

In this example, coherent displacement of rainfall features can be observed between the two rainfall fields. The estimated motion vectors align with this displacement, indicating that the optical flow method captures the dominant transport of rainfall structures across the domain. Such consistency provides empirical support for interpreting the estimated velocity field as an advection-consistent representation of rainfall motion.

Importantly, the purpose of this visualization is not to evaluate forecasting skill but to demonstrate that the estimated motion field provides a physically plausible description of rainfall transport over short time intervals.

https://doi.org/10.5194/egusphere-2026-1314
Preprint. Discussion started: 15 June 2026

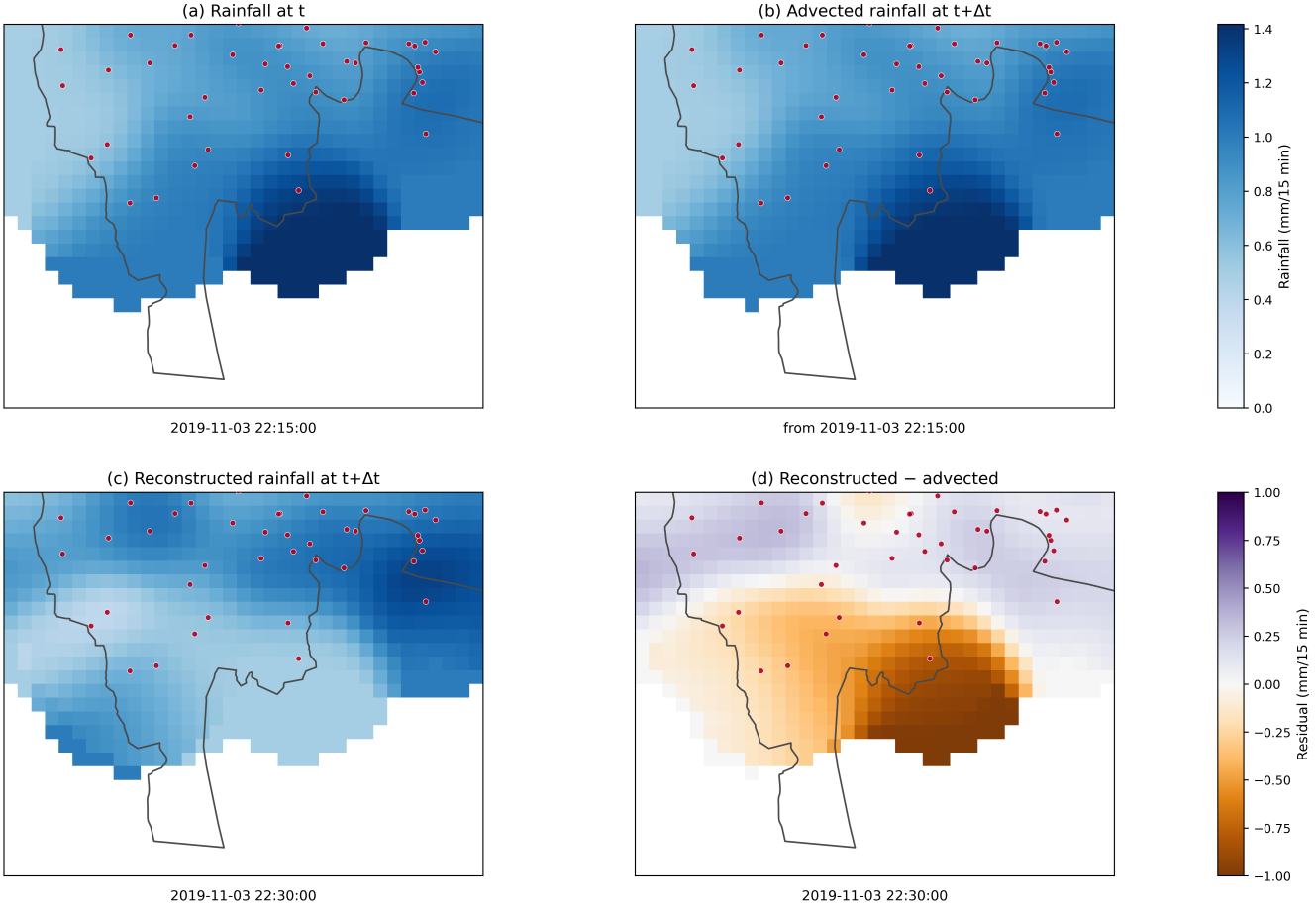

Figure 4. Example of advection-only rainfall evolution. (a) Gridded rainfall intensity field at time t derived from rain gauge observations. (b) Rainfall field advected from t to $t+\Delta t$ using the estimated motion field shown in Fig. 3 (b). (c) Gridded rainfall intensity field at time $t+\Delta t$ reconstructed from rain gauge observations. (d) Difference between the reconstructed and advected rainfall fields, highlighting regions where rainfall growth or decay occurs and where pure advection fails to fully explain the observed rainfall evolution.

The advection-only rainfall field therefore provides a physically interpretable reference state against which deviations from advection can be quantified. In the following section, these deviations are analyzed through the residual of the rainfall continuity equation.

6 Continuity-equation residual as a physics-based indicator

The motion field estimated in Section 5 describes the horizontal displacement of rainfall structures between consecutive time steps. This estimation is obtained using optical flow, which assumes that the observed rainfall field evolves primarily through

https://doi.org/10.5194/egusphere-2026-1314
Preprint. Discussion started: 15 June 2026

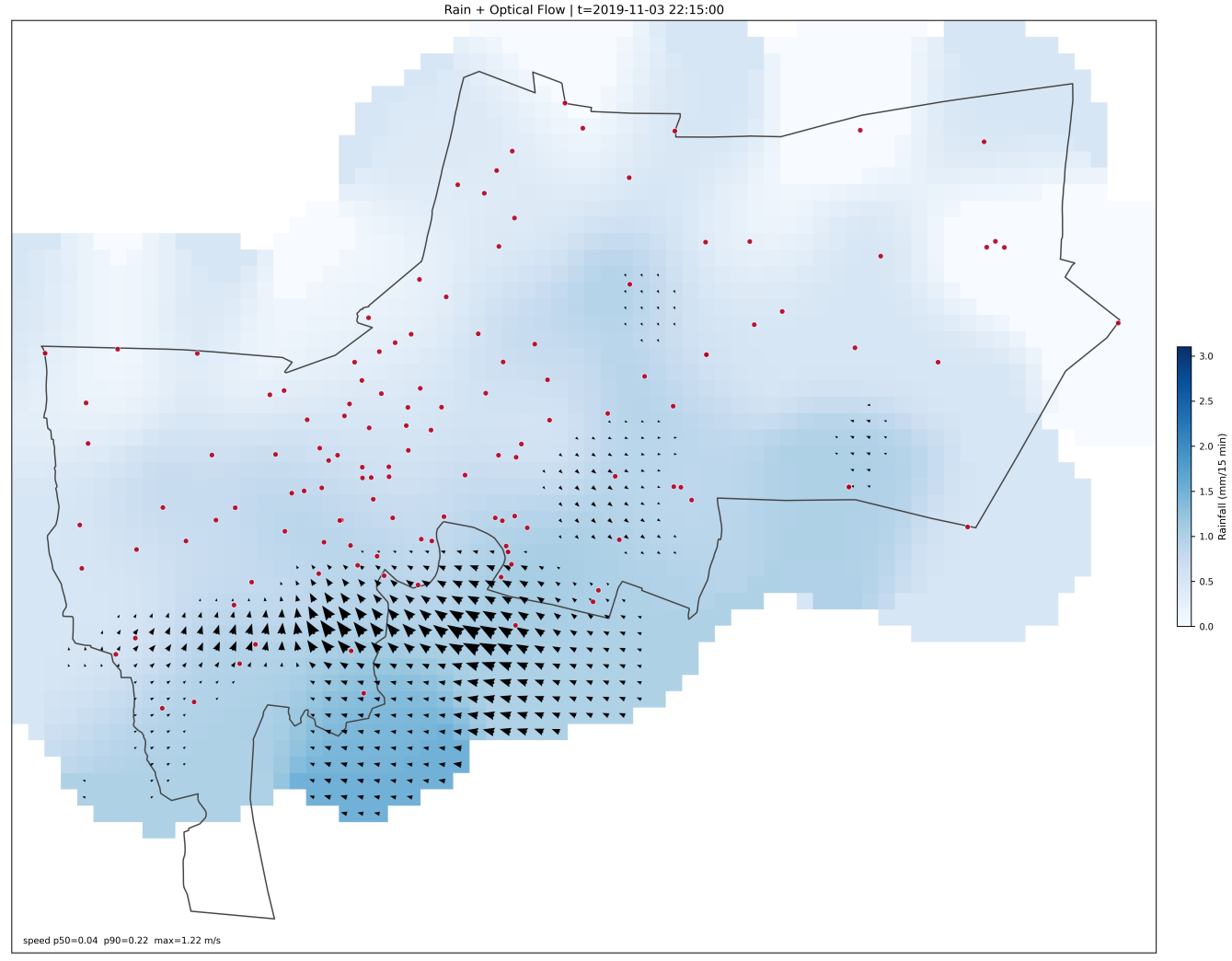

Figure 5. Example of the estimated rainfall motion field obtained using the Horn-Schunck optical flow method. The background color represents rainfall intensity, while arrows denote the horizontal velocity vectors (u, v) describing the displacement of rainfall structures between two consecutive observation times. The vector field exhibits spatially coherent motion patterns consistent with the advection of precipitation systems over the study area.

spatial transport. Under this assumption, rainfall intensity behaves approximately as a scalar quantity that is advected by a motion field.

This assumption can be written using a conservation framework. If rainfall intensity $R(x, y, t)$ is treated as a transported scalar field, its temporal evolution can be described by a continuity equation with a source-sink term,

$$\frac{\partial R}{\partial t} + \nabla \cdot (R\mathbf{u}) = S, \tag{3}$$

https://doi.org/10.5194/egusphere-2026-1314
Preprint. Discussion started: 15 June 2026

where $\mathbf{u} = (u, v)$ denotes the horizontal motion field estimated from optical flow and S represents local generation or decay processes that cannot be explained by horizontal transport.

Equation (3) provides a generalized description of rainfall evolution. The divergence term $\nabla \cdot (R\mathbf{u})$ represents changes in rainfall intensity due to spatial transport, while the source-sink term S accounts for internal atmospheric processes such as convective growth, microphysical decay, or local precipitation initiation.

In practice, the advective component of rainfall evolution can be approximated by transporting the rainfall field using the estimated motion field. This produces an advection-only rainfall field

$$R_{\mathrm{adv}}(x, y, t + \Delta t), \tag{4}$$

which represents the rainfall distribution expected at time $t + \Delta t$ if the rainfall structure observed at time t were displaced by the estimated motion field without local growth or decay.

Rainfall residuals are defined as the difference between the observed rainfall field and this advection-only rainfall field at the same time. In other words, the residual answers a direct diagnostic question: after moving the previous rainfall structure forward using the estimated motion field, where does the actually observed rainfall exceed or fall below that transport-based expectation? This deviation is quantified as

$$R_{\mathrm{res}}(x, y, t + \Delta t) = R_{\mathrm{obs}}(x, y, t + \Delta t) - R_{\mathrm{adv}}(x, y, t + \Delta t), \tag{5}$$

which we denote as the residual rainfall field R_{res}.

With this sign convention, positive residual values occur where the observed rainfall field is larger than the advected field, indicating local rainfall growth or development that cannot be explained by horizontal transport alone. Negative residual values occur where the observed field is smaller than the advected field, indicating rainfall weakening or dissipation relative to the transport-based reference. Persistent and spatially coherent positive residuals are therefore interpreted in this framework as measurement-based signatures of convective development.

Under a discrete time interval Δt, the residual can be interpreted as a practical approximation of the source-sink term in the continuity equation,

$$S(x, y, t) \approx \frac{R_{\mathrm{res}}(x, y, t + \Delta t)}{\Delta t}. \tag{6}$$

From this perspective, the residual field $R_{\mathrm{res}}(x, y, t+\Delta t)$ represents the portion of rainfall evolution that cannot be explained by horizontal advection. Regions with residual values near zero indicate rainfall structures that evolve consistently with the estimated motion field, whereas large positive residual values indicate locally generated or rapidly intensifying precipitation.

An example of this residual field is illustrated in Fig. 4 (d).

The residual field therefore provides the basis for the convective rainfall detection introduced in the next section.

https://doi.org/10.5194/egusphere-2026-1314
Preprint. Discussion started: 15 June 2026

7 Operational definition of convective rainfall

This section describes the operational framework used to identify convective rainfall systems within the observational rainfall dataset analyzed in this study. The objective of the framework is to translate the conceptual interpretation of rainfall evolution introduced in the previous section into a practical procedure applicable to high-resolution rainfall observations.

The analysis begins by organizing rainfall measurements into rainfall events at individual observation stations. These station-level events are then aggregated into storm-level event windows representing rainfall episodes affecting multiple stations within the study region.

For each storm-level event, rainfall evolution is examined using an advection-based representation of rainfall transport, which provides a physically interpretable reference describing how rainfall patterns would evolve under horizontal motion alone. This reference evolution serves as the baseline against which observed rainfall changes are evaluated.

Deviations between the observed rainfall evolution and the advection-consistent reference state are quantified through the residual of the rainfall continuity equation. Residual fields derived from this comparison capture rainfall changes that cannot be explained by horizontal transport alone.

From these residual fields, a set of storm-level indicators is derived to characterize the magnitude, spatial scale, and temporal persistence of non-advection-consistent rainfall evolution. These indicators form the basis for classifying rainfall systems into convective and non-convective storms.

The following subsections describe the definition of station rainfall events, the construction of storm-level events, the advection-based rainfall evolution model, the residual formulation, the residual-derived indicators, and the classification of convective storms.

7.1 Definition of station rainfall events

Rainfall events are defined independently at each observation station using the rainfall time series measured by rain gauges. The rainfall dataset used in this study is obtained from a rain-gauge network providing measurements at a temporal resolution of $15\,\mathrm{min}$ across the study area.

Let $R_{\mathrm{obs}}(\mathbf{x}, t)$ denote the observed rainfall intensity at station location $\mathbf{x}$ and time t. A rainfall occurrence is defined when $R_{\mathrm{obs}}(\mathbf{x}, t) > 0$.

Rainfall events are constructed by grouping successive rainfall occurrences in time. Two rainfall periods are considered part of the same event provided that the rainfall-free interval between them does not exceed $120\,\mathrm{min}$. When the dry interval exceeds this threshold, a new rainfall event is initiated.

Allowing short rainfall-free gaps prevents a single meteorological episode from being artificially fragmented due to brief interruptions in precipitation or measurement variability. Each station rainfall event is therefore represented as a continuous period of rainfall activity.

For each event, basic attributes are recorded, including the event start time, end time, duration, and accumulated rainfall amount.

https://doi.org/10.5194/egusphere-2026-1314
Preprint. Discussion started: 15 June 2026

These station-level rainfall events form the fundamental observational units used in the subsequent construction of storm-level rainfall systems described in the following subsection.

7.2 Construction of storm-level events

Rainfall events defined at individual stations represent local observations recorded by the rain-gauge network. During a rainfall episode, precipitation may be observed at multiple stations across the study area with partially overlapping or closely spaced time intervals. To construct regional-scale rainfall episodes for analysis, station-level events are therefore aggregated into storm-level events.

Storm construction is based on the temporal relationship among station rainfall events across the observation network. Station events are assigned to the same storm when their time intervals overlap or when the temporal separation between them is smaller than a predefined threshold of $120\,\mathrm{min}$. This rule allows rainfall occurrences recorded at different stations within a short time window to be associated with a common storm-level event window.

Small temporal gaps are permitted during the aggregation process. Allowing such gaps prevents a single rainfall episode from being artificially divided into multiple storms when rainfall temporarily ceases at some stations while continuing at others.

This temporal linkage rule is used as a practical way to construct analysis windows from point-based gauge observations in a compact urban domain with a 131-station rain-gauge network. The rule should not be interpreted as a claim that all rainfall observed during the window necessarily belongs to one isolated convective cell. Instead, it defines the time period over which the subsequent gauge-derived spatial fields, motion estimates, and residual indicators are evaluated.

Because storm identity is operational in this framework, the storm-level event should be interpreted as a rainfall-system window defined from the available gauge observations rather than as a unique external storm-object label. The adequacy of this event construction is assessed through the subsequent gauge-derived spatial fields, motion estimates, residual indicators, and physically plausible storm characteristics. Simultaneous rainfall systems in spatially separated parts of the domain may therefore be represented within the same analysis window; for larger domains or sparser gauge networks, additional spatial-connectivity criteria or integration with other observing systems may be useful.

Each resulting storm-level event is characterized by its overall duration and the set of stations reporting rainfall during the event.

This storm-level representation forms the analysis unit used in the subsequent examination of rainfall evolution. The construction procedure is applied to all station rainfall events detected in the observational dataset over the analysis period.

7.3 Advection-based rainfall evolution

To examine the evolution of rainfall systems over the study region, rainfall observations are represented as a spatial rainfall field varying in time. Let $R(x, y, t)$ denote the rainfall intensity at spatial location (x, y) and time t, obtained from the observational rainfall dataset. Successive rainfall fields describe the spatial distribution of precipitation at each observation time.

https://doi.org/10.5194/egusphere-2026-1314
Preprint. Discussion started: 15 June 2026

The horizontal movement of rainfall patterns between consecutive time steps is described by a velocity field

$$\mathbf{u}(x,y,t) = (u(x,y,t), v(x,y,t)),$$

which represents the displacement of rainfall structures over the analysis domain.

In this study, the motion field is estimated directly from the observed rainfall fields using optical-flow methods applied to successive time frames. Optical flow provides a spatially varying estimate of rainfall motion, allowing the translation of precipitation patterns to be inferred from changes in the rainfall distribution.

Using the estimated motion field, an advection-based rainfall field is constructed by transporting the rainfall field at time t forward by a time interval Δt. The resulting field, denoted as $R_{\mathrm{adv}}(x,y,t+\Delta t)$, represents the rainfall distribution expected at the next time step if precipitation structures were transported solely by horizontal motion.

This advection-only field serves as a reference representation of rainfall evolution driven purely by horizontal transport and is used in subsequent analysis to evaluate deviations between observed and transport-based rainfall evolution.

7.4 Residual of the rainfall continuity equation

Rainfall evolution over the study region can be expressed using the continuity equation for a scalar field transported by a horizontal velocity field. In two spatial dimensions, the rainfall continuity equation is written as

$$\frac{\partial R}{\partial t} + \nabla \cdot (R\mathbf{u}) = S, \tag{7}$$

where $R(x,y,t)$ denotes rainfall intensity, $\mathbf{u}(x,y,t)$ is the horizontal motion field describing rainfall transport, and $S(x,y,t)$ represents source or sink processes associated with local rainfall generation or dissipation.

To evaluate rainfall evolution in the observational dataset, the observed rainfall field at time $t+\Delta t$ is compared with the advection-based rainfall field obtained from the transport model. Let $R_{\mathrm{obs}}(x,y,t+\Delta t)$ denote the observed rainfall field and $R_{\mathrm{adv}}(x,y,t+\Delta t)$ the rainfall field predicted by horizontal advection of the previous rainfall field.

The rainfall residual is defined as the observed field minus the advected field,

$$R_{\mathrm{res}}(x,y,t+\Delta t) = R_{\mathrm{obs}}(x,y,t+\Delta t) - R_{\mathrm{adv}}(x,y,t+\Delta t). \tag{8}$$

This residual provides a diagnostic measure of rainfall evolution that cannot be explained by horizontal transport alone. Positive residual values indicate rainfall growth relative to the transport-based reference, while negative residual values correspond to rainfall weakening or decay. Persistent and spatially coherent positive residuals are used here as signatures of convective rainfall development.

7.5 Residual-based convective indicators

Residual fields derived from the rainfall dataset contain spatial and temporal patterns reflecting rainfall evolution that cannot be explained by horizontal transport alone. To characterize these patterns at the storm level, a set of quantitative indicators is computed from the residual fields associated with each storm event.

https://doi.org/10.5194/egusphere-2026-1314
Preprint. Discussion started: 15 June 2026

These indicators summarize key properties of residual structures observed during the evolution of a rainfall system, including their intensity, spatial extent, and temporal persistence. The indicators are derived directly from the residual fields calculated for each analysis time step.

The following indicators are evaluated for every storm event:

- **Peak positive residual area:** the maximum spatial area of contiguous grid cells exhibiting positive residual values within the storm duration.
- **Peak residual intensity:** the largest positive residual value observed within a single time frame of the storm.
- **Event-integrated positive residual:** the cumulative positive residual summed over all grid cells and time steps throughout the storm duration.
- **Number of strong residual frames:** the number of time steps in which the residual field exceeds a predefined threshold indicating substantial rainfall growth beyond transport-based evolution.

These indicators characterize three fundamental aspects of non-advection-consistent rainfall evolution: the magnitude of rainfall change, the spatial scale of residual structures, and the persistence of these structures over time.

The indicators are examined jointly to evaluate their ability to distinguish convective storms from transport-dominated rainfall systems. As shown in the following sections, indicators related to the spatial extent and temporal persistence of positive residual structures provide the strongest separation between storm types, whereas peak residual intensity alone shows weaker discriminative power.

7.6 Convective storm classification

Storm systems are classified into convective and non-convective categories using the residual-based indicators computed for each storm event.

Exploratory analysis of the indicator distributions reveals that metrics describing the spatial extent and persistence of positive residual structures provide the most robust separation between storm types. In particular, the peak positive residual area, the event-integrated positive residual, and the number of strong residual frames consistently distinguish storms exhibiting strong local rainfall growth from storms whose evolution is largely explained by horizontal transport.

Based on these observations, the classification rule focuses on the spatial and temporal characteristics of positive residual structures. Positive residual cells are first identified using $R_{\mathrm{res}} \geq 0.2$, and strong positive residual cells are identified using $R_{\mathrm{res}} \geq 0.5$. A storm is classified as convective when its peak positive-residual area is at least 500 grid cells and at least one of the following supporting criteria is also satisfied:

- peak positive residual sum of at least 1000,
- event-integrated positive residual of at least 4000, or

https://doi.org/10.5194/egusphere-2026-1314
Preprint. Discussion started: 15 June 2026

– at least 10 strong residual frames.

Strong residual frames are frames containing at least three rainy cells and at least three cells exceeding the strong positive-residual threshold. These conditions indicate rainfall growth patterns that cannot be reproduced by transport-based rainfall evolution alone and therefore represent signatures of convective rainfall generation.

Storms that do not satisfy these conditions generally exhibit weaker and less persistent residual structures and are categorized as non-convective precipitation systems.

Section 8 examines the resulting statistical separation between convective and non-convective storms in the residual-indicator feature space.

8 Diagnostic behavior of detected convective storms

This section evaluates whether the residual-based framework produces storm classifications with physically interpretable diagnostic behavior. The purpose is not to present a standalone rainfall climatology for Bangkok, but to test whether storms identified from the residual indicators show characteristics expected for convective rainfall systems.

Across the analyzed dataset, a total of 157 storm episodes were identified, of which 36 (22.9%) were classified as convective and 121 (77.1%) as non-convective. Despite representing a smaller fraction of the storm population, convective storms exhibit systematically stronger signatures in the residual-based feature space, including larger positive-residual footprints, stronger event-scale residual accumulation, and more persistent residual activity.

The convective classification described in Section 7.6 is implemented using threshold values derived from the empirical distributions of the residual indicators. In particular, the peak positive-residual area provides the clearest separation between storm types and is used as the primary threshold variable in the rule-based classification. Storms whose peak residual area exceeds the threshold are identified as convective, while additional indicators such as the event-integrated positive residual and the number of strong residual frames provide supporting evidence of sustained rainfall growth.

The following subsections examine these characteristics in more detail. Storm-scale statistics are first analyzed to compare the structural properties of convective and non-convective storms. The distribution of residual-based indicators is then evaluated to illustrate how the two storm classes occupy different regions in the residual feature space.

8.1 Seasonal and diurnal distribution

To examine whether the detected convective storms exhibit realistic temporal patterns, the occurrence of storms was analyzed jointly by month and hour of day. This temporal analysis is used as a physical plausibility check on the residual-based classification rather than as the primary objective of the study. A total of 157 storm episodes were identified in the dataset, among which 36 storms (22.9%) were classified as convective and 121 storms (77.1%) as non-convective.

Figure 6 shows the joint distribution of storm initiation times across months and hours of the day. Storm occurrences are strongly concentrated in the late rainy-season months of October to December, with the largest number of events observed in

https://doi.org/10.5194/egusphere-2026-1314
Preprint. Discussion started: 15 June 2026

November. This seasonal concentration is consistent with rainfall-seasonality studies in monsoon regions (Mu et al., 2021; Gu et al., 2025).

Beyond the seasonal concentration, storms occur preferentially during the afternoon to evening period. Most storm initiations occur between approximately 15:00 and 20:00 local time, with the strongest concentration around the early evening hours. Such timing corresponds closely to the typical diurnal cycle of convective rainfall, where daytime surface heating can support increasing atmospheric instability and convective development later in the afternoon (Nakaegawa et al., 2019; Mu et al., 2021; Gu et al., 2025).

The combined seasonal-diurnal structure therefore indicates that the storms identified by the residual-based framework follow physically plausible occurrence patterns rather than appearing randomly across time.

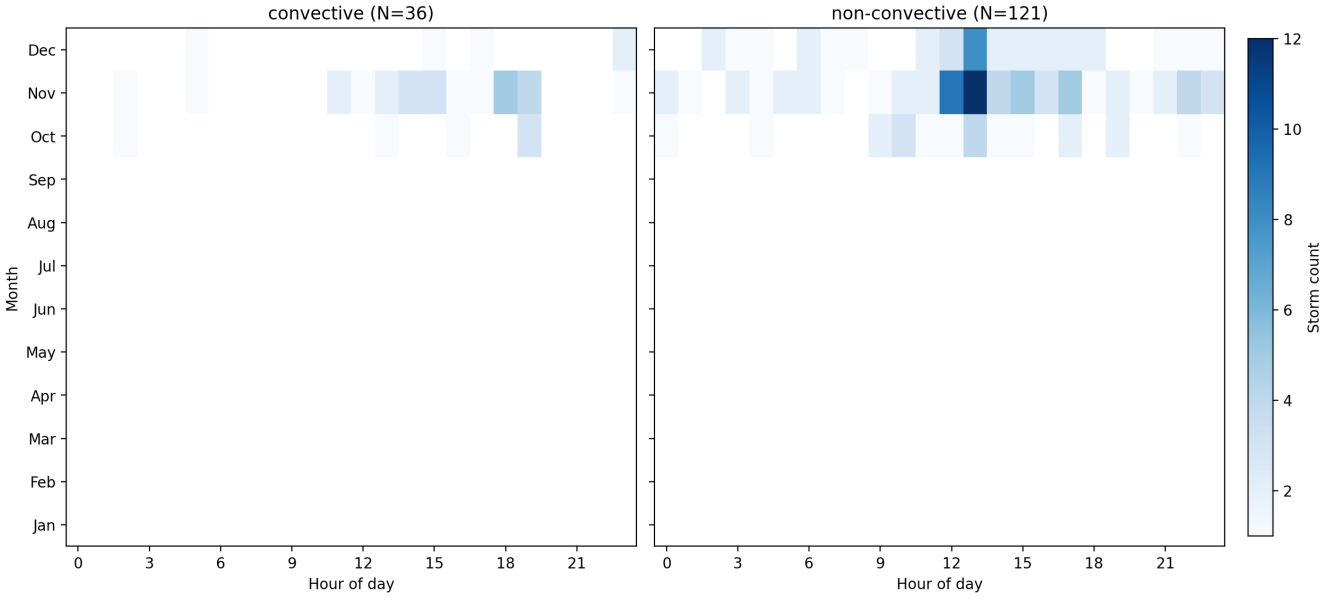

Figure 6. Joint distribution of storm initiation times by month and hour of day. Storm occurrences are concentrated in the late rainy-season months (October–December) and occur most frequently during the late afternoon to early evening hours, consistent with the typical seasonal and diurnal cycle of tropical convective rainfall.

8.2 Diurnal characteristics

While the seasonal-diurnal heatmap in Fig. 6 summarizes the overall temporal distribution of storms, it is also informative to examine how convective and non-convective storms differ in their diurnal timing. Convective storms detected by the residual-based framework exhibit a clear late-afternoon to evening preference. The hourly distribution of storm start times is shown in Fig. 7, where storm initiation times are grouped by hour of day using the labeled storm dataset obtained from the residual-based classification.

https://doi.org/10.5194/egusphere-2026-1314
Preprint. Discussion started: 15 June 2026

Non-convective storms occur throughout the day, with a noticeable concentration around the midday period (approximately 12:00–14:00). In contrast, convective storms become more frequent during the late afternoon and early evening hours. The number of convective storms begins to increase after approximately 14:00 and reaches its highest levels around 18:00–19:00 local time.

This shift toward later hours indicates that storms characterized by strong positive residual signatures tend to occur after the peak surface heating period. Such timing is consistent with the typical diurnal evolution of tropical convection, where atmospheric instability develops during the afternoon and convective activity intensifies toward the evening.

Overall, the observed diurnal structure supports the physical interpretation of the residual-based classification: storms identified as convective tend to occur later in the day than storms dominated by advection-consistent rainfall evolution.

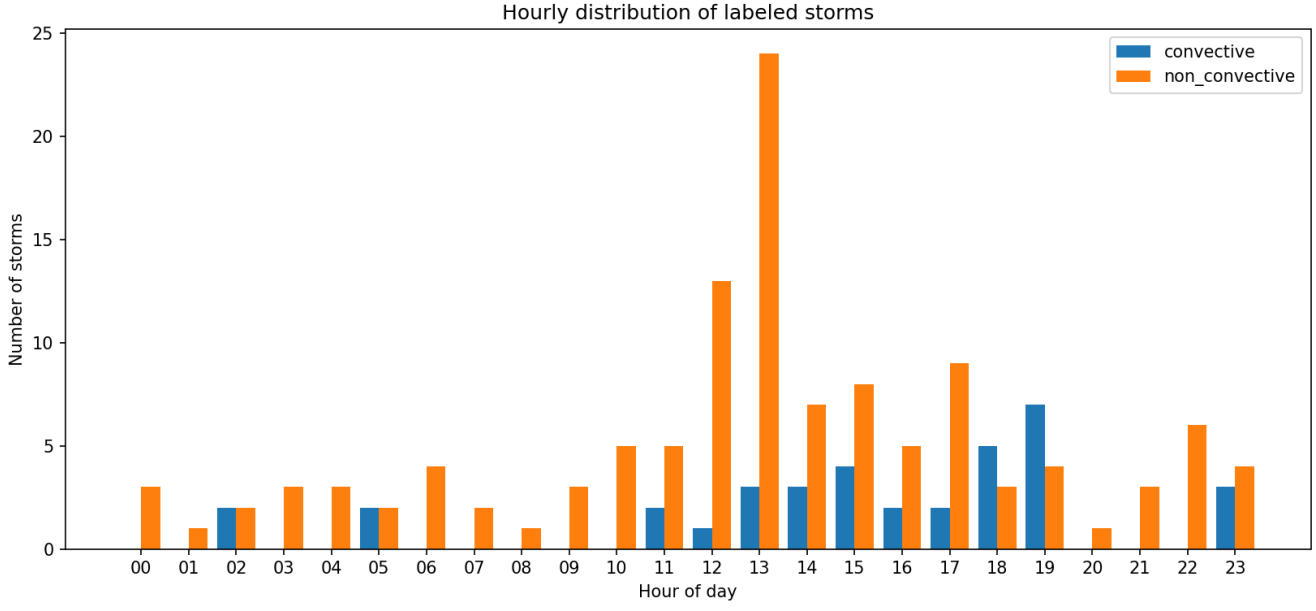

Figure 7. Hourly distribution of storm initiation times by storm type. Non-convective storms occur throughout the day with a noticeable midday concentration, whereas convective storms occur preferentially during the late afternoon and early evening hours.

8.3 Spatial footprint

Figure 8 compares several residual-based metrics between convective and non-convective storms. These metrics quantify the spatial extent, cumulative magnitude, and temporal persistence of positive residual signatures derived from the rainfall continuity equation.

The clearest separation between the two storm types appears in the *peak positive-residual area* (Fig. 8 (a)), which represents the maximum number of grid cells exhibiting positive residuals within a storm. Convective storms show substantially larger

https://doi.org/10.5194/egusphere-2026-1314
Preprint. Discussion started: 15 June 2026

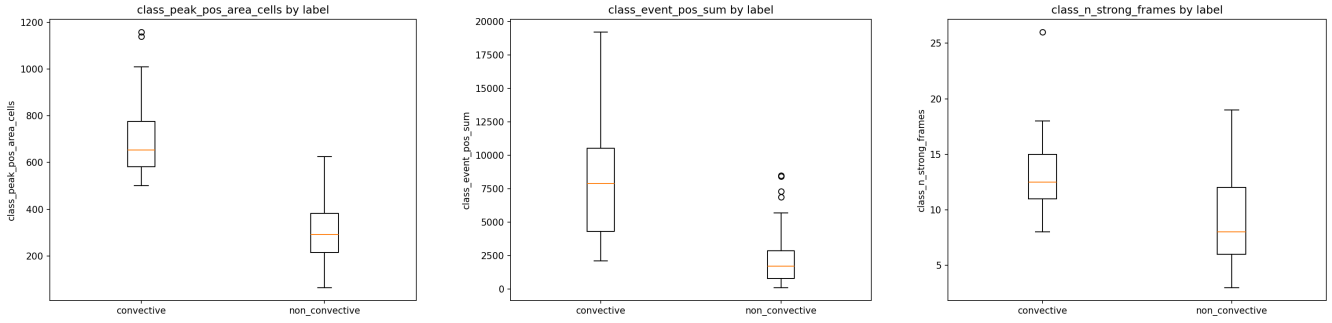

(a) **(b)** **(c)**

Figure 8. Distributions of three residual-based storm indicators for convective and non-convective storms: (a) peak positive-residual area (maximum number of grid cells with positive residuals within a storm), (b) event-integrated positive residual rainfall, and (c) number of strong-residual frames. Convective storms consistently exhibit larger residual footprints, greater cumulative residual rainfall, and longer persistence of strong residual activity compared with non-convective storms.

residual footprints, with a median peak area of approximately 650 cells and an interquartile range of roughly 580–770 cells. In contrast, non-convective storms exhibit a median of about 290 cells with an interquartile range of approximately 210–380 cells. The limited overlap between these distributions indicates that convective storms tend to produce much larger spatial regions of rainfall growth that cannot be explained by horizontal advection alone.

A similar but more dispersed separation is observed in the *event-scale positive residual sum* (Fig. 8 (b)). Convective storms exhibit a median value of roughly 8,000 with an interquartile range of about 4,300–10,500, whereas non-convective storms show a median near 1,700 and an interquartile range of approximately 800–2,800. Although the separation remains substantial, the spread of the distribution is larger because this metric accumulates residual contributions across the entire storm lifecycle.

The temporal persistence of strong residual signals is illustrated by the *number of strong-residual frames* (Fig. 8 (c)). Convective storms typically contain around 12 strong frames (IQR ≈11–15), whereas non-convective storms show a median near 8 frames (IQR ≈ 6–12). This difference suggests that convective storms not only produce stronger residual signatures but also maintain them for longer periods during their evolution.

Overall, the results indicate that convective storms are characterized by larger spatial footprints of positive residuals, greater cumulative residual magnitudes, and longer persistence of strong residual activity. Among these metrics, the peak positive-residual area provides the most distinct separation between storm types, highlighting the importance of spatially organized rainfall growth as a key indicator of convective processes.

https://doi.org/10.5194/egusphere-2026-1314
Preprint. Discussion started: 15 June 2026

8.4 Residual statistics

Convective storms identified by the proposed framework exhibit systematically stronger positive residual signatures than non-convective storms. Because the residual represents rainfall growth that cannot be explained by horizontal advection alone, these differences provide a direct physical indication of convective development.

Table 2 summarizes the principal residual indicators for the two storm classes. Convective storms consistently exhibit larger spatial residual footprints, stronger accumulated residual magnitudes, and more persistent residual activity than non-convective storms.

Table 2. Residual indicators for convective and non-convective storms (median values). Convective storms exhibit substantially stronger and more persistent positive residual signatures.

Metric	Convective	Non-convective
Peak positive residual area (median cells)	654.5	292
Event-integrated positive residual (median)	7872.5	1686.2
Strong residual frames (median)	12.5	8

8.4.1 Residual feature-space separation

The three residual indicators collectively define a residual feature space describing the spatial extent, accumulated magnitude, and temporal persistence of rainfall generation beyond advection.

Across all three indicators, convective storms consistently occupy higher-value regions of this feature space. The spatial footprint of positive residual rainfall is substantially larger for convective storms, with a median peak residual area of about 655 cells compared with approximately 292 cells for non-convective storms.

The magnitude of rainfall generation beyond advection shows an even stronger contrast. The median event-integrated positive residual reaches about 7,872 for convective storms but only about 1,686 for non-convective storms, indicating much stronger storm-integrated rainfall growth.

Temporal persistence also differs systematically between the two classes. Convective storms exhibit a median of 12.5 strong residual frames, whereas non-convective storms typically show about 8 frames, suggesting that convective development tends to remain active for longer portions of the storm lifecycle.

Taken together, these differences indicate that convective storms occupy a distinct region of the residual feature space, characterized by larger spatial residual footprints, stronger accumulated residual magnitudes, and more persistent residual activity.

https://doi.org/10.5194/egusphere-2026-1314
Preprint. Discussion started: 15 June 2026

8.4.2 Persistence of residual signatures

Convective storms also exhibit substantially stronger temporal persistence of positive residual activity. Measured by the number of time steps exceeding the strong-residual threshold, convective storms contain on average 12.9 strong residual frames (median 12.5 time steps), whereas non-convective storms show mean and median values of 9.0 and 8 frames, respectively.

This contrast indicates that the residual signatures associated with convective rainfall are temporally coherent rather than isolated noise spikes. Convective rainfall growth therefore tends to occur as sustained local generation processes rather than short-lived fluctuations in the rainfall field.

The persistence of residual activity is further reflected in the structure of the residual feature space shown in Fig. 9. The panels illustrate the relationships between the spatial footprint of positive residual rainfall and three complementary indicators: the event-integrated positive residual, the number of strong residual frames, and the peak residual intensity.

Across all panels, convective storms extend toward regions characterized by both larger residual footprints and stronger residual magnitudes, whereas non-convective storms remain concentrated near smaller residual values. This structural pattern indicates that convective storms are associated with spatially coherent and temporally persistent regions of rainfall generation beyond advection-consistent transport.

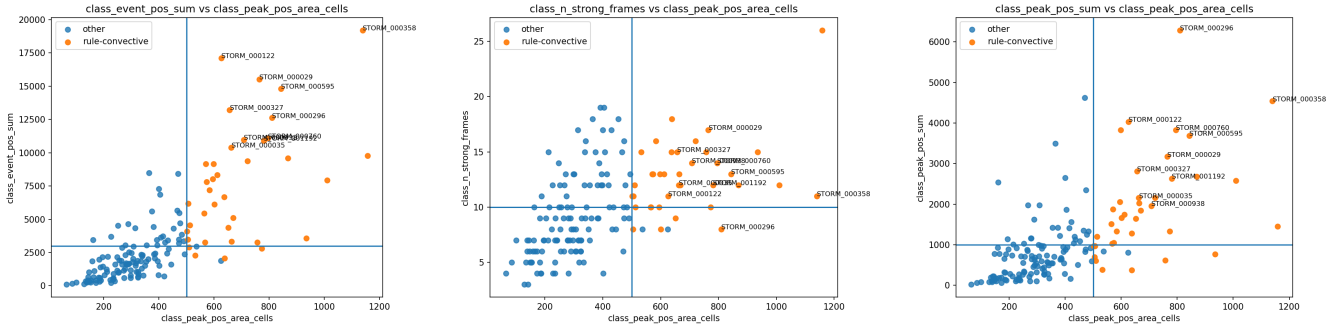

(a) **(b)** **(c)**

Figure 9. Residual feature-space representation of detected storms. Each panel shows the relationship between the spatial footprint of positive residual rainfall and a complementary residual indicator. Convective storms tend to occupy regions characterized by both larger residual magnitudes and larger spatial footprints, whereas non-convective storms remain concentrated near smaller residual values. The vertical line indicates the peak residual-area threshold (approximately 500 grid cells) used in the rule-based convective classification.

8.4.3 Residual accumulation

A further contrast between the two storm classes is observed in the total positive residual accumulated over the lifetime of each storm. Convective storms produce a mean event-integrated positive residual of 8008.6 (median 7872.5), whereas non-convective storms show a mean of 2045.0 and a median of 1686.2.

https://doi.org/10.5194/egusphere-2026-1314
Preprint. Discussion started: 15 June 2026

The accumulated residual therefore provides a storm-scale measure of integrated rainfall generation beyond advection-consistent transport, and further supports the use of the residual term as a physically interpretable feature for identifying convective rainfall systems.

9 Conclusions

9.1 Physical implications

This study introduces a physics-informed definition of convective rainfall based on deviations from rainfall evolution consistent with horizontal advection. Using the rainfall continuity equation, rainfall change is interpreted as the combination of two components: (i) advection-consistent transport of existing precipitation structures and (ii) internally generated changes that cannot be explained by advection alone.

Within this framework, convective rainfall is not defined by high intensity alone, but by the emergence of rainfall in locations where the advection-only evolution of the rainfall field does not predict its occurrence. Statistical analysis in Section 8 shows that events classified as convective exhibit characteristics such as larger residual footprints, stronger residual accumulation, and greater temporal persistence, which are consistent with documented properties of convective systems, including rapid initiation, spatial localization, and strong association with the afternoon diurnal heating cycle (Wang et al., 2021; Li et al., 2024; Gu et al., 2025).

This deviation corresponds conceptually to the source term in the rainfall continuity equation, $\frac{\partial R}{\partial t} + \nabla \cdot (R\mathbf{u}) = S$, where the computed residual can be interpreted as a diagnostic proxy for S under the assumption that short-term rainfall transport is reasonably approximated by horizontal advection.

An important implication of this formulation is that convective initiation can be analyzed using rain-gauge observations alone. Rain-gauge networks are typically regarded as insufficient for studying convective dynamics due to their sparse spatial coverage. However, the presence of physically consistent seasonal and diurnal signatures in the residual-based classification suggests that meaningful dynamical information about convective behavior can be extracted from surface rainfall observations when combined with a physics-based framework.

9.2 Comparison with intensity-based definitions

Many existing approaches classify convective rainfall using intensity thresholds (e.g., rainfall rate in $\mathrm{mm, hr^{-1}}$), radar texture features, or supervised learning techniques. These approaches are useful for operational classification, but they are generally empirical and not directly linked to governing equations describing rainfall evolution.

The framework proposed here differs conceptually by focusing on dynamical consistency with advection rather than rainfall magnitude. Rainfall of moderate intensity that appears abruptly in localized regions may therefore be identified as convective. Conversely, heavy rainfall that is continuously advected from upstream without local initiation may not be classified as convective under this definition.

https://doi.org/10.5194/egusphere-2026-1314
Preprint. Discussion started: 15 June 2026

The objective of the proposed approach is not to replace intensity-based definitions, but to complement them. By distinguishing between rainfall generated locally and rainfall transported from upstream, the method provides additional physical insight into rainfall dynamics.

9.3 Limitations

Despite its physical interpretability, several limitations should be noted.

First, the motion field estimated using optical flow represents a kinematic approximation of rainfall motion. Rapid microphysical changes occurring within the same observation interval may therefore contribute to the residual, making it difficult to fully separate model limitations from genuine dynamical processes.

Second, the spatial resolution of the reconstructed rainfall field depends directly on rain-gauge density. This limitation follows from the gauge-derived field representation: when inter-station spacing approaches or exceeds the typical size of convective cells, the ability to resolve localized rainfall initiation is expected to decrease.

Accordingly, the proposed framework should be regarded as a dense-network method rather than a general sparse-gauge method. In the Bangkok network used here, the median nearest-neighbor spacing among geolocated stations is approximately 1.5 km, but station spacing is not spatially uniform across the full metropolitan domain. The applicability of the framework therefore depends on local station spacing, spatial coverage, and the representativeness of gauge locations. Application to sparse networks would require additional validation or integration with other observing systems before the residual field can be interpreted as evidence of localized rainfall generation.

Third, the framework assumes that linear advection provides a reasonable approximation of rainfall transport over short time intervals. For longer time horizons, nonlinear storm evolution and deformation of rainfall structures may reduce the validity of this assumption.

Finally, because the analysis relies solely on surface rainfall observations, the method does not provide direct information about vertical structure or microphysical processes within convective systems.

9.4 Applicability to other cities

The proposed advection-consistency framework is not specific to Bangkok. Provided that a sufficiently dense rain-gauge network is available to construct kilometer-scale rainfall fields with temporal resolution on the order of 10–15 unitmin, the same methodology can be applied to other tropical or subtropical urban regions.

Key requirements include: (i) sufficiently dense spatial coverage to estimate rainfall motion, (ii) temporally consistent observations, and (iii) reliable measurement quality.

Under these conditions, the framework is expected to identify convective behavior characterized by localized rainfall initiation and strong diurnal modulation, which are common features of convective precipitation in tropical environments.

Future work integrating this framework with weather radar observations or high-resolution numerical models may enable direct comparison between surface residual signatures and vertical convective dynamics, providing a pathway toward linking surface rainfall observations with dynamical interpretations of convective development.

https://doi.org/10.5194/egusphere-2026-1314
Preprint. Discussion started: 15 June 2026

Code availability. The analysis code used in this study was developed for the specific experimental framework of this work. Access to the code may be provided by the corresponding author upon reasonable request for research purposes.

Data availability. The rainfall gauge data used in this study were provided by the Bangkok Metropolitan Administration. Due to data-sharing policies, the data are not publicly available but may be obtained from the data provider subject to permission from the Bangkok Metropolitan Administration.

Author contributions. Punpiti Piamsa-nga: Conceptualization, Methodology, Software, Data curation, Investigation, Formal analysis, Visualization, Writing – original draft preparation. Nalina Phisanbut: Methodology, Formal analysis, Visualization, Writing – review and editing. Napaporn Piamsa-nga: Conceptualization, Supervision, Scientific interpretation of meteorological processes, Writing - review and editing. All authors discussed the results and contributed to the final manuscript.

Competing interests. The authors declare that they have no competing interests.

Disclaimer. Large language models (ChatGPT and Gemini) were used for language refinement and limited assistance in code drafting. All scientific ideas, analysis, and conclusions are the responsibility of the authors.

Acknowledgements. The authors thank the Department of Drainage and Sewerage, Bangkok Metropolitan Administration, for providing the rain-gauge observations used in this study. This work was supported by the Kasetsart University Research and Development Institute under grant number FF (KU) 36.67.

https://doi.org/10.5194/egusphere-2026-1314
Preprint. Discussion started: 15 June 2026

References

Abbasi, A., Kambali, P. N., Shahidi, P., and Nataraj, C.: Physics-Informed Machine Learning for Modeling Multidimensional Dynamics, Nonlinear Dynamics, 112, 21 565–21 585, https://doi.org/10.1007/s11071-024-10163-3, 2024.

Anagnostou, E. N.: A convective/stratiform precipitation classification algorithm for volume scanning weather radar observations, Meteorological Applications, 11, 291–300, https://doi.org/10.1017/s1350482704001409, 2004.

Berne, A. and Krajewski, W. F.: Radar for hydrology: Unfulfilled promise or unrecognized potential?, Advances in Water Resources, 51, 357–366, https://doi.org/10.1016/j.advwatres.2012.05.005, 2013.

Bhasme, P., Vagadiya, J., and Bhatia, U.: Enhancing predictive skills in physically-consistent way: Physics Informed Machine Learning for hydrological processes, Journal of Hydrology, 615, 128 618, https://doi.org/10.1016/j.jhydrol.2022.128618, 2022.

Bowler, N. E., Pierce, C. E., and Seed, A.: Development of a precipitation nowcasting algorithm based upon optical flow techniques, Journal of Hydrology, 288, 74–91, https://doi.org/10.1016/j.jhydrol.2003.11.011, quantitative Precipitation Forecasting II, 2004.

Caseri, A. N., Lima Santos, L. B., and Stephany, S.: A convolutional recurrent neural network for strong convective rainfall nowcasting using weather radar data in Southeastern Brazil, Artificial Intelligence in Geosciences, 3, 8–13, https://doi.org/10.1016/j.aiig.2022.06.001, 2022.

Das, P., Posch, A., Barber, N., Hicks, M., Duffy, K., Vandal, T., Singh, D., Werkhoven, K. v., and Ganguly, A. R.: Hybrid physics-AI Outperforms Numerical Weather Prediction for Extreme Precipitation Nowcasting, npj Climate and Atmospheric Science, 7, 282, https://doi.org/10.1038/s41612-024-00834-8, 2024.

Das, S., Chakraborty, R., and Maitra, A.: A random forest algorithm for nowcasting of intense precipitation events, Advances in Space Research, 60, 1271–1282, https://doi.org/10.1016/j.asr.2017.03.026, 2017.

Feidas, H. and Giannakos, A.: Classifying Convective and Stratiform Rain Using Multispectral Infrared Meteosat Second Generation Satellite Data, Theoretical and Applied Climatology, 108, 613–630, https://doi.org/10.1007/s00704-011-0557-y, 2012.

Giannakos, A. and Feidas, H.: Classification of Convective and Stratiform Rain Based on the Spectral and Textural Features of Meteosat Second Generation Infrared Data, Theoretical and Applied Climatology, 113, 495–510, https://doi.org/10.1007/s00704-012-0802-z, 2013.

Gu, Y., Peng, D., Gong, Y., Fan, Z., Wang, T., Pang, B., and Ye, A.: Diurnal variation features and dry times impact based on the latest hourly satellite-based precipitation data across China, Journal of Hydrology: Regional Studies, 62, 102 859, https://doi.org/10.1016/j.ejrh.2025.102859, 2025.

Ha, J.-H. and Lee, H.: A Deep Learning Model for Precipitation Nowcasting Using Multiple Optical Flow Algorithms, Weather and Forecasting, 39, 41 – 53, https://doi.org/10.1175/waf-d-23-0104.1, 2024.

He, Z., Yang, Y., Fang, R., Zhou, S., Zhao, W., Bai, Y., Li, J., and Wang, B.: Integration of shapley additive explanations with random forest model for quantitative precipitation estimation of mesoscale convective systems, Frontiers in Environmental Science, Volume 10 - 2022, https://doi.org/10.3389/fenvs.2022.1057081, 2023.

Horn, B. K. and Schunck, B. G.: Determining optical flow, Artificial Intelligence, 17, 185–203, https://doi.org/10.1016/0004-3702(81)90024-2, 1981.

Karpatne, A., Atluri, G., Faghmous, J. H., Steinbach, M., Banerjee, A., Ganguly, A., Shekhar, S., Samatova, N., and Kumar, V.: Theory-Guided Data Science: A New Paradigm for Scientific Discovery from Data, IEEE Transactions on Knowledge and Data Engineering, 29, 2318–2331, https://doi.org/10.1109/tkde.2017.2720168, 2017.

Kashinath, K., Mustafa, M., Albert, A., Wu, J.-L., Jiang, C., Esmaeilzadeh, S., Azizzadenesheli, K., Wang, R., Chattopadhyay, A., Singh, A., Manepalli, A., Chirila, D., Yu, R., Walters, R., White, B., Xiao, H., Tchelepi, H. A., Marcus, P., Anandkumar, A., Hassanzadeh, P.,

https://doi.org/10.5194/egusphere-2026-1314
Preprint. Discussion started: 15 June 2026

and Prabhat: Physics-informed machine learning: case studies for weather and climate modelling, Philosophical Transactions of the Royal Society A: Mathematical, Physical and Engineering Sciences, 379, 20200 093, https://doi.org/10.1098/rsta.2020.0093, 2021.

Lazri, M. and Ameur, S.: Combination of support vector machine, artificial neural network and random forest for improving the classification of convective and stratiform rain using spectral features of SEVIRI data, Atmospheric Research, 203, 118–129, https://doi.org/10.1016/j.atmosres.2017.12.006, 2018.

Li, D., Qi, Y., and Li, H.: Statistical characteristics of convective and stratiform precipitation during the rainy season over South China based on GPM-DPR observations, Atmospheric Research, 301, 107 267, https://doi.org/10.1016/j.atmosres.2024.107267, 2024.

Li, H., Wang, X., Choy, S., Jiang, C., Wu, S., Zhang, J., Qiu, C., Zhou, K., Li, L., Fu, E., and Zhang, K.: Detecting heavy rainfall using anomaly-based percentile thresholds of predictors derived from GNSS-PWV, Atmospheric Research, 265, 105 912, https://doi.org/10.1016/j.atmosres.2021.105912, 2022a.

Li, H., Wang, X., Choy, S., Wu, S., Jiang, C., Zhang, J., Qiu, C., Li, L., and Zhang, K.: A New Cumulative Anomaly-Based Model for the Detection of Heavy Precipitation Using GNSS-Derived Tropospheric Products, IEEE Transactions on Geoscience and Remote Sensing, 60, 1–18, https://doi.org/10.1109/tgrs.2021.3137014, 2022b.

Luo, Y., Fang, S., Wu, B., Wen, Q., and Sun, L.: Physics-Guided Learning of Meteorological Dynamics for Weather Downscaling and Forecasting, in: Proceedings of the 31st ACM SIGKDD Conference on Knowledge Discovery and Data Mining V.2, KDD '25, pp. 2010–2020, Association for Computing Machinery, New York, NY, USA, ISBN 9798400714542, https://doi.org/10.1145/3711896.3737081, 2025.

Mu, X., Huang, A., Wu, Y., Xu, Q., Zheng, Y., Lin, H., Fang, D., Zhang, X., Tang, Y., and Cai, S.: Characteristics of the Precipitation Diurnal Variation and Underlying Mechanisms Over Jiangsu, Eastern China, During Warm Season, Frontiers in Earth Science, Volume 9 - 2021, https://doi.org/10.3389/feart.2021.703071, 2021.

Muñoz, C., Wang, L.-P., and Willems, P.: Enhanced object-based tracking algorithm for convective rain storms and cells, Atmospheric Research, 201, 144–158, https://doi.org/10.1016/j.atmosres.2017.10.027, 2018.

Nakaegawa, T., Pinzon, R., Fabrega, J., Cuevas, J. A., De Lima, H. A., Cordoba, E., Nakayama, K., Batista Lao, J. I., Lau Melo, A., Gonzalez, D. A., and Kusunoki, S.: Seasonal changes of the diurnal variation of precipitation in the upper Río Chagres basin, Panamá, PLOS ONE, 14, 1–22, https://doi.org/10.1371/journal.pone.0224662, 2019.

Smith, J., Birch, C., Marsham, J., Peatman, S., Bollasina, M., and Pankiewicz, G.: Evaluating pySTEPS optical flow algorithms for convection nowcasting over the Maritime Continent using satellite data, Natural Hazards and Earth System Sciences, 24, 567–582, https://doi.org/10.5194/nhess-24-567-2024, 2024.

Teufel, B., Carmo, F., Sushama, L., Sun, L., Khaliq, M. N., Bélair, S., Shamseldin, A., Kumar, D. N., and Vaze, J.: Physics-Informed Deep Learning Framework to Model Intense Precipitation Events at Super Resolution, Geoscience Letters, 10, 19, https://doi.org/10.1186/s40562-023-00272-z, 2023.

Villarini, G. and Krajewski, W. F.: Review of the Different Sources of Uncertainty in Single Polarization Radar-Based Estimates of Rainfall, Surveys in Geophysics, 31, 107–129, https://doi.org/10.1007/s10712-009-9079-x, 2010.

Wang, Y., Tang, L., Chang, P.-L., and Tang, Y.-S.: Separation of convective and stratiform precipitation using polarimetric radar data with a support vector machine method, Atmospheric Measurement Techniques, 14, 185–197, https://doi.org/10.5194/amt-14-185-2021, 2021.

Xiao, C., Yuan, W., and Yu, R.: Diurnal cycle of rainfall in amount, frequency, intensity, duration, and the seasonality over the UK, International Journal of Climatology, 38, 4967–4978, https://doi.org/10.1002/joc.5790, 2018.

https://doi.org/10.5194/egusphere-2026-1314
Preprint. Discussion started: 15 June 2026

Xie, K., Liu, P., Zhang, J., Han, D., Wang, G., and Shen, C.: Physics-guided deep learning for rainfall-runoff modeling by considering extreme events and monotonic relationships, Journal of Hydrology, 603, 127 043, https://doi.org/10.1016/j.jhydrol.2021.127043, 2021.

Zhao, D., Dong, W., Lin, Y., Hu, Y., and Cao, D.: Diurnal Variation of Precipitation over the High Mountain Asia: Spatial Distribution and Its Seasonality, Journal of Hydrometeorology, 23, 1945 – 1959, https://doi.org/10.1175/jhm-d-21-0243.1, 2022.

Zhao, Z., Wang, Z., Zhao, G., and Zhao, J.: A New Strong Convective Precipitation Forecasting Method Based on Attention Mechanism and Spatio-Temporal Reasoning, Scientific Reports, 14, 19 024, https://doi.org/10.1038/s41598-024-68951-1, 2024.

Zhong, Q., Zhang, Z., Yao, X., Hou, S., Fu, S., Cao, Y., and Jing, L.: Improved Forecasting via Physics-Guided Machine Learning as Exemplified Using "21·7" Extreme Rainfall Event in Henan, Science China Earth Sciences, 67, 1652–1674, https://doi.org/10.1007/s11430-022-1302-1, 2024.

Zhuo, H., Zhao, P., and Zhou, T.: Diurnal cycle of summer rainfall in Shandong of eastern China, International Journal of Climatology, 34, 742–750, https://doi.org/10.1002/joc.3718, 2014.